ELSEVIER

Ceramics International 33 (2007) 273–278

CERAMICS INTERNATIONAL

www.elsevier.com/locate/ceramint

Preparation and characterization of indium-doped tin oxide thin films

P.K. Manoj [a], Benny Joseph [b], V.K. Vaidyan [a], D. Sumangala Devi Amma [c,*]

[a] *Department of Physics, University of Kerala, Thiruvananthapuram 695 581, India*
[b] *Department of Physics, St. Joseph's College, Calicut 673 008, India*
[c] *Department of Physics, TKM College of Arts & Science, Kollam 691 005, India*

Received 16 June 2005; received in revised form 7 July 2005; accepted 19 September 2005
Available online 27 December 2005

Abstract

Highly transparent and semiconducting indium-doped tin oxide films were prepared by spray pyrolysis. These films were characterized by X-ray diffraction, scanning electron microscopy, energy dispersive spectroscopy and optical transmission. X-ray diffraction studies have shown the polycrystalline nature of the films. The preferential orientations as well as the electro-optical properties are sensitive to indium doping. The structural, electrical and optical studies carried out on these films reveal their columnar and compact structure.

Keywords: Indium-doped tin oxide; Thin films; Spray pyrolysis

1. Introduction

Tin oxide (SnO_2) is a wide band gap n-type semiconductor, which can be efficiently used as transparent conducting oxide. Because of its unique electrical and optical properties, tin oxide thin films have been widely used in photocell devices and optoelectronic displays [1]. The electrical conductivity of undoped SnO_2 is in the range of 1.1–350 Ω^{-1} cm^{-1} depending on the method of preparation [2]. Addition of appropriate amounts of dopants such as antimony, fluorine and bromine remarkably enhances the electrical conductivity [3]. The addition of indium, an acceptor impurity, to tin oxide increases the resistivity but enhances the transmittance [4]. The optical transmittance of SnO_2 together with its chemical and mechanical stability makes SnO_2 films suitable for many applications such as transparent conductive coatings, gas sensors and heterojunction solar cells. Reactively evaporated indium-doped SnO_2 (SnO_2:In) thin films were found to be sensitive to nitric oxide, NO [5].

The methods that are used more often for depositing SnO_2 are sputtering [2], evaporation [6], chemical vapour deposition [7,8], sol–gel process [9,10] and pyrolysis of stannic compounds [11–13]. Of these methods, spray pyrolysis represents the less expensive alternative. Indium doping to tin oxide films is very rare in literature. In the present study, indium-doped tin oxide films have been prepared by spray pyrolysis technique and the effect of doping in the structural, electrical and optical properties are discussed.

2. Experimental details

Thin films of SnO_2:In were deposited on glass substrates (soda lime, 3.5 cm × 2.5 cm × 0.1 cm) using the spray pyrolysis coating unit and the experimental setup is described elsewhere [14]. By using absolute ethanol, 0.1 M stannic chloride (99.99%) solution was prepared. A little HCl was added to the solution. To achieve indium doping, indium chloride ($InCl_3$, 99.99%) was added to the precursor solution. The amount of $InCl_3$ to be added depends on the desired doping concentration. The indium doping concentration was varied from 0 to 10 at.%. The optimum deposition parameters, which are summarized in Table 1, are attained by trial and error method. The solution was sputtered by airflow onto heated glass substrates held at a constant temperature of 425 °C in a furnace, in which the temperature of the substrate during the spray could be controlled within ±5 °C with the help of a temperature controller. The substrate to nozzle distance was kept at 40 ± 1 cm. Compressed air was used as the carrier gas. To enhance electrical conductivity, the above deposited films were annealed at 400 °C for 1 h under a vacuum of 10^{-5} mbar.

* Corresponding author.
E-mail address: sumachittor@yahoo.com (D.S.D. Amma).

0272-8842/$32.00
doi:10.1016/j.ceramint.2005.09.016

Table 1
Optimum conditions for the spray deposited indium-doped tin oxide films

Spray parameters	Optimum value/suitable item
Solution concentration	0.1 M
Precursor	$SnCl_4{\cdot}5H_2O$, $InCl_3$
Solvent	Absolute ethanol
Substrate temperature	425 ± 5 °C
Carrier gas	Compressed air (2 kg/cm^2)
Substrate to nozzle distance	40 ± 1 cm
Rate of spray	4.8 ± 0.1 mL/min
Time of spray	10 min
Dopant concentration	2 at.%

Crystallinity and phase analysis of the films were carried out with Philips 1830 X-ray diffraction spectrometer, with an accelerating potential of 40 kV and a current of 30 mA, using Cu Kα radiation (0.154056 nm), which is equipped with Ni filter. All peaks were recorded at a scanning rate of 1° min^{-1} in steps of 0.03° in the standard θ–2θ geometry. Data was acquired over $2\theta = 20$–70° range. The film thickness was measured by multiple beam interferometric method and was found to be 170 nm for all films. The surface morphology of the films and elemental analysis were performed with JEOL JSM 5600 LV scanning electron microscope fitted with an energy dispersive spectrometer. The resistivity of the films was measured by the four-probe method. Optical transmission of the films was obtained in the wavelength range 300–800 nm with an Ocean Optics PC 1000 spectrometer.

3. Results and discussion

3.1. X-ray diffraction studies

X-ray diffraction spectra recorded on SnO_2:In films with different indium concentrations deposited at a substrate temperature of 425 ± 5 °C using 0.1 M stannic chloride are shown in Fig. 1. The crystal structure of the sprayed films is generally the same as that of the corresponding bulk material. This may not be the case, however, when the material components are formed during pyrolysis. The presence of SnO, a meta-stable phase, also abundance of Sn^{2+}, O_2^- and small amount of Cl^- ions have been reported in SnO_2 films [15,16]. In the present investigation, all the peaks in the pattern correspond to tetragonal rutile structure of SnO_2 and are indexed on the basis of JCPDS file No. 41–1445. However, the relative intensity of the individual reflections does not agree with the JCPDS data. This is because of the fact that the films studied were of finite thickness (170 nm) for Cu Kα radiation, where as JCPDS data give relative intensities for powder specimen which are of infinite thickness. No phase corresponding to indium, indium oxide or any other indium compound was detected in the XRD patterns. Undoped SnO_2 films have shown a preferential orientation along (2 0 0) crystal plane at the optimized deposition conditions [13]. It is quite clear from the XRD spectra that all the films are polycrystalline and highly oriented along (2 0 0) plane up to an In content of 5 at.%. Presence of other orientations such as (1 1 0), (1 0 1), (2 1 1), (2 2 0) and (3 1 0) have also been detected. But no other crystalline phases were detected.

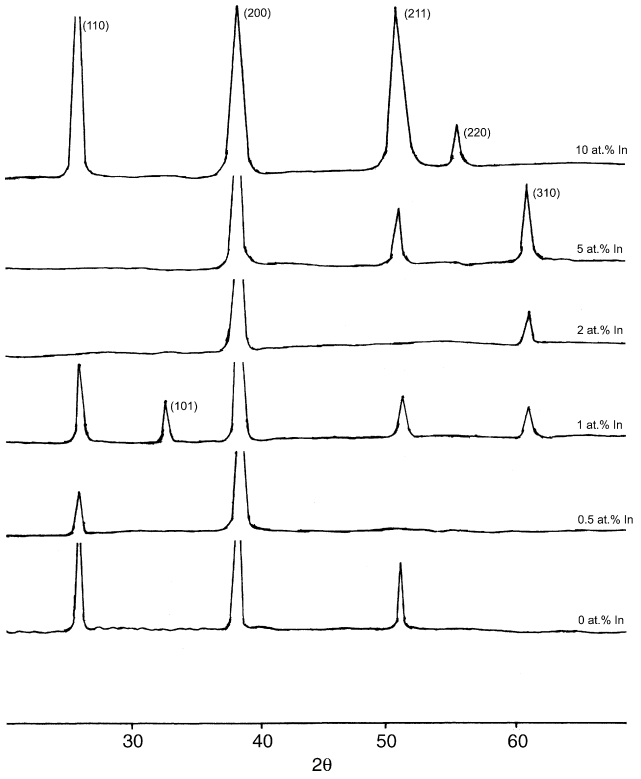

Fig. 1. X-ray diffractograms of indium-doped tin oxide films with different indium concentration.

In the high doping level, at 10 at.% of indium, the preferential orientation is changed to (1 1 0) and the intensity of (2 0 0) plane decreases. The lattice parameters calculated from the most prominent peaks are found to be in agreement with JCPDS values. The crystallite size along a line normal to the preferentially oriented crystal plane is calculated using Scherrer's formula [17]

$$D = \frac{0.9\lambda}{B\cos\theta} \quad (1)$$

where θ is the Bragg's diffraction angle; B, the broadening of diffraction line at half its maximum intensity; and λ, the wavelength of X-rays. The lattice parameter values (a and c) and crystallite size (D) of these samples are tabulated in Table 2. From the table it is evident that nanograins form

Table 2
Structural parameters of indium-doped tin oxide thin films

Indium concentration (at.%)	Lattice parameters		Crystallite size (nm)
	a (nm)	c (nm)	
0	0.4719	0.3201	15.9
0.5	0.4708	–	9.6
1	0.4718	0.3216	9.2
2	0.4716	–	8.7
5	0.4719	0.3221	7.6
10	0.4706	0.3251	7.2
JCPDS (41–1445)	0.4737	0.3187	

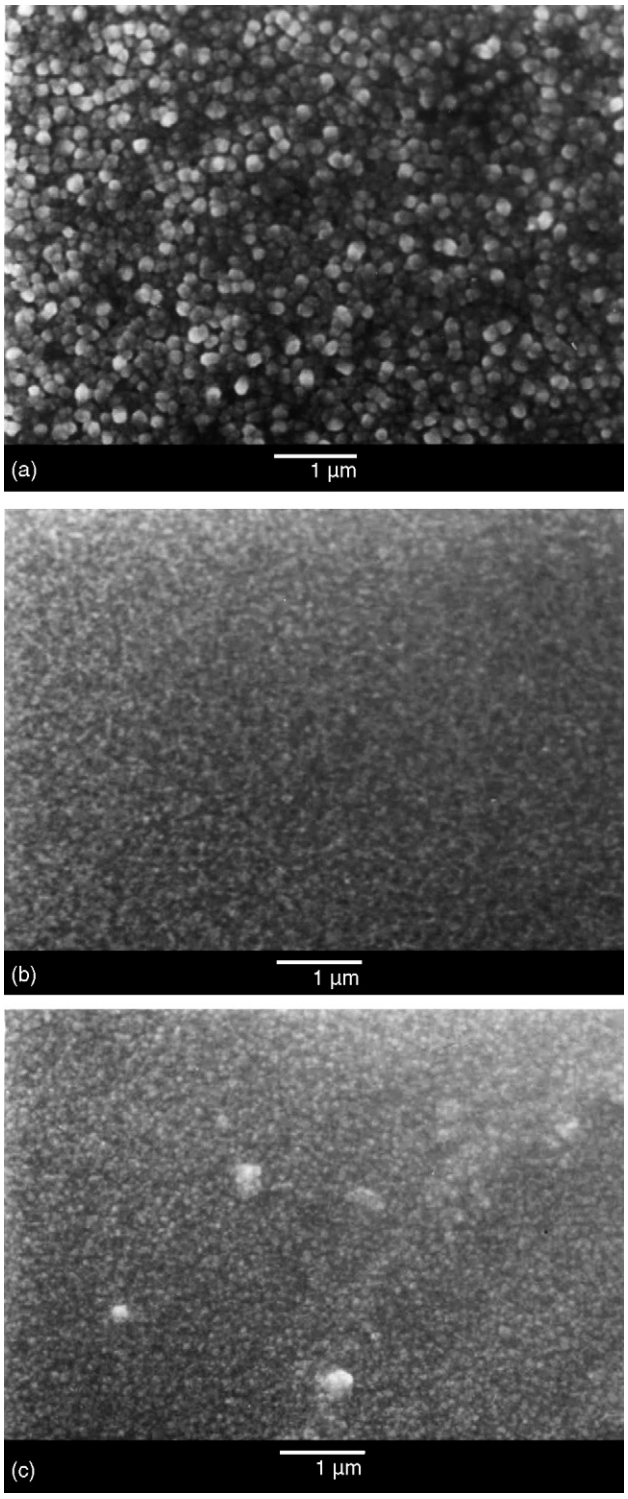

Fig. 2. SEM photographs of indium-doped tin oxide films (a) 0, (b) 2 and (c) 10 at% In.

the films. This result is consistent with SEM studies. The crystallite sizes are found to decrease with the dopant concentration. This may probably due to the effect of recrystallization process because of doping.

3.2. SEM and EDS studies

Fig. 2 shows the scanning electron micrographs of the sample deposited at 0, 2 and 10 at.% of indium-doped SnO_2 films. It is observed that all the films are smooth, devoid of pinholes and consist of well-defined crystallites. There is significant change in the crystallite size due to indium doping. It can be seen from Fig. 2(a–c) that the grain size decreases as the doping level increases from 0 to 10 at.% of In doping. Moreover, the micrograph of the film doped with 10 at.% In shows densely packed small grains.

Energy dispersive spectroscopy was used for the qualitative analysis of 0, 2 and 10 at.% In doped samples. They revealed the presence of Sn, In and O from their characteristic X-rays. The most remarkable result is that the presence of chlorine is not detected in any of the samples. If the pyrolytic reactions have not been completed, some by-products or intermediate compounds would have been trapped as impurities in the film. In the case of chloride salts, residual chlorine is often obtained in the films [18].

3.3. Optical and electrical studies

Optical constants of thin films are, however, influenced by various factors such as the substrate temperature, film thickness, crystallinity, nature and amount of dopants. These factors also affect the electrical properties of thin films.

The transmission in the wavelength range 300–800 nm for indium-doped SnO_2 films are shown in Fig. 3. The transmission increases up to 2 at.% doped sample. Films doped with 0.5–2 at.% In show interference effect. This is a direct evidence of homogenous film with uniform thickness [19]. The interference fringes are the result of interference of the light reflected between the air-film and film-substrate interfaces. For heavily doped samples, 5 and 10 at.%, transmittance decreases. For 2 at.% In doped sample, transmittance improves significantly from the undoped one. The smooth surface and the small crystallite size observed in the SnO_2:In films produce less

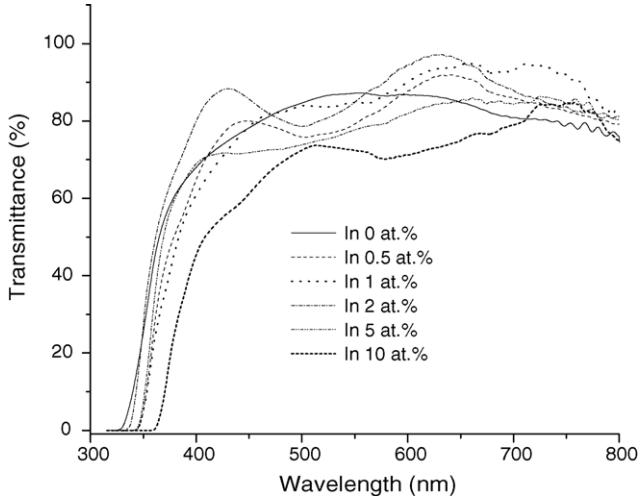

Fig. 3. Transmission spectra of SnO_2:In films with different indium concentrations.

scattering effects. Hence, the films have a larger optical transmittance than those obtained for undoped films. For 10 at.% doped sample even though the crystallite sizes are still smaller as seen from the SEM observations, the transmittance decreases. The decrease of transmittance at higher doping concentrations may be due to the increased scattering of photons by crystal defects created by doping.

Optical properties of any material are characterized by two parameters, i.e., refractive index n and extinction coefficient k. From the transmission spectrum alone the refractive index of the films can be calculated using envelope method [20]

$$n = [N + (N^2 - s^2)^{1/2}]^{1/2} \tag{2}$$

and

$$N = \frac{1+s^2}{2} + \frac{8s^2}{(1+s)^2}\frac{T_M - T_m}{T_M T_m}$$

where s is the refractive index of the substrate, T_M and T_m are maximum and minimum transmittance, respectively, for a particular wavelength, obtained by drawing an envelope in the transmittance spectrum. The extinction coefficient is also calculated as described below in the visible range of the spectrum using the relation

$$k = \frac{\alpha\lambda}{4\pi} \tag{3}$$

where α is calculated from the equation

$$x = \exp(-\alpha t) \tag{4}$$

where

$$x = \frac{E_M - [E_M^2 - (n^2-1)^3(n^2-s^4)]^{1/2}}{(n-1)^3(n-s^2)}$$

$$E_M = \frac{8n^2 s}{T_M} + (n^2-1)(n^2-s^2).$$

Fig. 4 shows the plot of refractive index and extinction coefficient as a function of wavelength λ for 2 at.% indium-doped SnO_2 film. The refractive index is found to decrease with wavelength; this behaviour $dn/d\lambda < 0$, is consistent with what one would expect from Kramers–Kroning analysis [21]. The extinction coefficient values are in the range as predicted from the envelope method ($k < 0.05$). The low value of extinction coefficient indicates the low surface roughness of the prepared sample. Porosity of the sample doped with 2 at.% In is calculated using the Lorentz–Lorenz equation and the values are found to be less than 1% [22].

No material is fully transparent in all optical frequencies and hence there will always be some absorption in some region of the spectra. In the strong absorption region, absorption coefficient α can be calculated from Lambert's formula,

$$\alpha = \frac{1}{t}\ln\left(\frac{1}{T}\right) \tag{5}$$

where T and t are transmittance and film thickness, respectively.

The absorption has its minimum at low energy and increases with optical energy in a manner similar to the absorption edge of the semiconductors. The absorption coefficient α for directly allowed transition for simple parabolic scheme can be ascribed as a function of incident photon energy as

$$\alpha h\upsilon \propto (h\upsilon - E_g)^{1/2} \tag{6}$$

where E_g is the optical band gap.

The optical band gap is calculated from $(\alpha h\upsilon)^2$ versus $h\upsilon$ graph.

Fig. 5 indicates the variation of $(\alpha h\upsilon)^2$ with $h\upsilon$ for In doped tin oxide films prepared in the present study. It is observed that In doping increases the band gap slightly for low doping levels, and the values are tabulated in Table 3.

The effect of In content on the sheet resistance of SnO_2:In films was studied. It is observed that indium addition increases the sheet resistance significantly. On SnO_2 surfaces, the indium atoms act as surface acceptors, increasing the Schottky barrier and decreasing the conductance [5]. In the present investigation, the sheet resistance increased to nearly seven times when only 0.5 at.% of In was added. When the doping level is

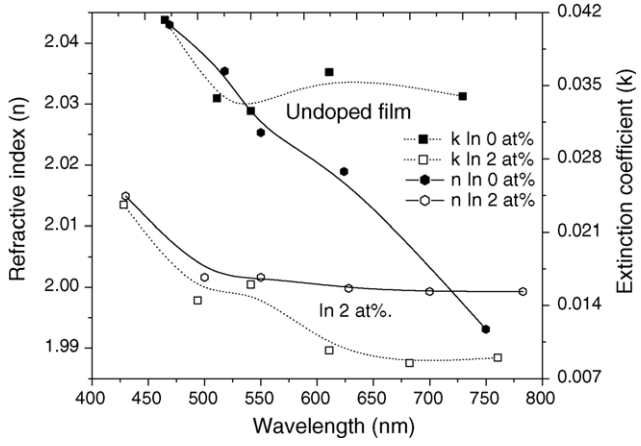

Fig. 4. Variation of refractive index and extinction coefficient with wavelength for undoped and 2 at.% In doped tin oxide films.

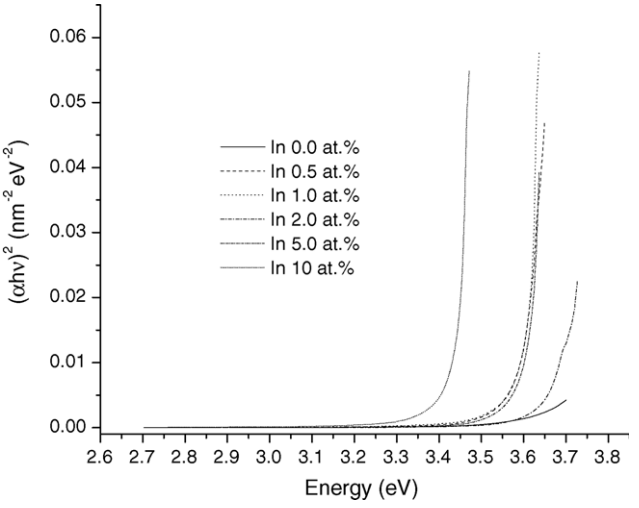

Fig. 5. Variation of $(\alpha h\upsilon)^2$ with photon energy for SnO_2:In films with different In concentrations.

Table 3
Electrical and optical properties of indium-doped tin oxide films

Concentration of indium (at.%)	Sheet resistance		Resistivity after vacuum annealing ($\times 10^{-3}$ Ωm)	Transmittance at 550 nm (%)	Optical band gap (eV)
	As-deposited (kΩ/□)	Vacuum annealed (kΩ/□)			
0	0.49	0.179	0.0292	87.2	3.58
0.5	6.38	1.24	0.21	79.5	3.59
1	40.7	16	2.7	84.8	3.6
2	139	24	4.1	84.8	3.66
5	521	111	18.8	77.4	3.55
10	1628	435	73.9	72.5	3.46

increased form 0.5 to 10 at.%, the sheet resistance of the films increases from 6.3 to 1638 kΩ/□. The as-deposited films were annealed at 400 °C for 1 h under a vacuum of 10^{-5} mbar. The sheet resistance of 0.5 at.% indium-doped films decreased to 1.24 kΩ/□ from 6.38 kΩ/□ due to vacuum annealing. This reduction is attributed to the desorption of oxygen from the films. The original resistance can be recovered by subsequent heating in air/oxygen. The process of adsorption and desorption is completely reversible. Indium-doped SnO_2 films show a variation of resistivity from 1.2×10^{-4} to 6×10^{-5} Ωm on vacuum annealing at 350 °C [23]. The as-deposited value of resistivity is restored by annealing in air at 400 °C. Rohatgi et al. [24] reported an increase of sheet resistance by four orders of magnitude when only 3 mol.% In was added. They also reported that the initial additions of group III (indium, thallium) and group V (antimony, phosphorous) oxides had strikingly opposite effects on sheet resistance, with In and Sb having the most pronounced effects. Large additions of Sb, P, Tl and In increased the resistance and activation energy and reduced the charge carrier concentration. According to them these effects are probably associated with the observed increased disorder and altered crystallographic orientation in the films. In the present study, the preferred orientation changes from (2 0 0) to (1 1 0) when the doping level was increased to 10 at.%. The sheet resistance, resistivity, transmittance and band gap, of indium-doped tin oxide films are summarized in Table 3. The resistivity is found to increase with dopant concentration. But maximum transmittance is obtained for 2 at.% doped sample. The resistivity obtained for the 2 at.% doped sample is 4.1×10^{-3} Ωm.

The addition of a small amount of doping elements to SnO_2 thin films has been known to be effective in modifying their optical and electrical properties [25]. In particular, in the case of gas sensor applications, a general strategy for tailoring materials for the selective sensor response involves the modification of the surface by the addition of dopants during sensor fabrication. Hence, there is a growing interest in doping SnO_2 with different elements [26]. In the present study, we observed a decrease in grain size due to indium doping. The grain size of the samples prepared is of the order of 7–9 nm. In experimental and theoretical works, grain size effects on the sensitivity of gas sensor devices have been reported [27]. The experimental studies revealed that the sensitivity is enhanced when the grain size is decreased. Also Xu et al. [28] have observed that, by reducing the particle size (∼6 nm), high gas sensitivity and short response times can be achieved. From the study of indium-doped SnO_2 films, it has been concluded that uniform, homogenous and highly transparent films with small grain size can be prepared by indium doping on tin oxide. But the films are highly resistive. Hence, SnO_2:In coatings can be used in areas where only a moderate electronic conductivity is required.

4. Conclusions

Indium-doped tin oxide films were deposited by spray pyrolysis technique utilizing an ethanolic solution containing $SnCl_4 \cdot 5H_2O$ and $InCl_3$. Also, the effect of increasing indium concentration on the electrical, optical and structural properties of the films had been studied. The optical measurements show that the transmittance improves with increasing indium content from 0 to 2 at.%. However, with more increasing indium content, the transmittance decreases. But the sheet resistance of the films was found to increase with indium concentrations. As evidenced from X-ray diffraction analysis, SnO_2:In films prepared at 425 ± 5 °C with various indium concentrations are polycrystalline. It also indicates that for low doping levels up to 5 at.%, the preferred orientation of crystallites is along (2 0 0) which is same as that for undoped films. But for a doping level of 10 at.%, the preferred orientation changes to (1 1 0). The crystallite sizes are found to decrease with indium doping. SEM observations also indicate a smooth surface morphology with small grains for the films studied. This result may be particularly useful for gas sensing, as the sensitivity in gas detection improves with small grain size.

References

[1] G.W. Hunter, C.-C. Liu, D.B. Makel, in: M.-G. Hak (Ed.), The MEMS Hand Book, CRC Press, 2002 (chapter 22, pp. 22-1–22-24).
[2] B. Stjerna, E. Olssan, C.G. Granquist, J. Appl. Phys. 76 (1994) 3797.
[3] S. Supothina, R. Mark, De. Guire, Thin Solid Films 371 (2000) 1.
[4] K.L. Chopra, R.C. Kainth, D.K. Pandya, A.P. Thakoor, Chemical solution deposition of inorganic films, in: G. Hass, M.H. Francombe, J.L. Vossen (Eds.), Physics of Thin Films Advances in Research and Development, 12, Academic Press, New York, 1982.
[5] G.S. Sberveglieri, S. Groppelli, P. Nelli, Sens. Actuators, B 1 (1990) 79.
[6] M.H.M. Reddy, S.R. Jawalekar, A.W. Chandorkar, Thin Solid Films 169 (1989) 117.
[7] H. Kin, H.A. Laitinen, J. Am. Ceram. Soc. 58 (1975) 23.
[8] S.R. Vishwakarma, J.P. Upadhyay, H.C. Prasad, Thin Solid Films 176 (1989) 99.

[9] A. Maddalena, R.D. Maschio, S. Dire, A. Raccanelli, J. Non-Cryst. Solids 121 (1990) 365.
[10] J.P. Chatelon, C. Terrier, E. Bernstein, R. Berjoan, J.A. Roger, Thin Solid Films 247 (1994) 162.
[11] E. Shanthi, A. Banerjee, K.L. Chopra, J. Appl. Phys. 51 (1981) 6243.
[12] V. Vasu, A. Subrahmanyam, Thin Solid Films 202 (1991) 283.
[13] D.S.D. Amma, V.K. Vaidyan, P.K. Manoj, Mater. Chem. Phys. 93 (2005) 194.
[14] B. Joseph, K.G. Gopchandran, P.V. Thomas, P. Koshy, V.K. Vaidyan, Mater. Chem. Phys. 58 (1999) 71.
[15] J.C. Manifacier, L. Szepessy, J.F. Bresse, M. Perotin, R. Stuck, Mater. Res. Bull. 14 (1979) 109.
[16] D. Elliott, D.L. Zellner, H.A. Laitiner, J. Electrochem. Soc. 117 (1970) 1343.
[17] B.D. Cullity, Elements of X-ray Diffraction, Addison-Wesley Inc., Reading, 1978.
[18] J. Aranovich, A. Ortiz, R.H. Bube, J. Vac. Sci. Technol. 16 (1979) 994.
[19] R. Swanepoel, J. Phys. E. Sci. Instrum. 16 (1983) 1214.
[20] C.H. Peng, S.B. Desu, J. Am. Ceram. Soc. 77 (1994) 929.
[21] B. Sasi, K.G. Gopchandran, P.K. Manoj, P. Koshy, P.P. Rao, V.K. Vaidyan, Vacuum 68 (2003) 149.
[22] Y. Ohya, H. Saiki, T. Tanaka, Y. Takahashi, J. Am. Ceram. Soc. 79 (1996) 825.
[23] K.L. Chopra, S. Major, D.K. Pandya, Thin Solid Films 102 (1983) 1.
[24] A. Rohatgi, T.R. Viverito, L.H. Slack, J. Am. Ceram. Soc. 57 (1974) 278.
[25] D.J. Goyal, C. Agashe, B.R. Maratha, M.G. Takwale, V.G. Bhide, J. Appl. Phys. 73 (1993) 7250.
[26] P.A. Kox, R.G. Egdell, C. Harding, A.F. Orchard, W.R. Patterson, P.J. Tavener, Solid State Commun. 44 (1982) 837.
[27] M. Ippommatsu, H. Ohnishi, H. Saskaki, T. Matsumoto, J. Appl. Phys. 69 (1991) 836.
[28] C. Xu, J. Tamaki, N. Miura, N. Yamazoe, Sens. Actuators, B 3 (1991) 147.